

A High-Resolution Very Large Array Observation of a Protostar in OMC-3: Shock-induced X-ray Emission by a Protostellar Jet

Masahiro TSUJIMOTO,¹ Katsuji KOYAMA,² Naoto KOBAYASHI,³ Masao SAITO,⁴ Yohko TSUBOI,⁵
and

Claire J. CHANDLER⁶

¹*Department of Astronomy & Astrophysics, Pennsylvania State University,
525 Davey Laboratory, University Park, PA 16802, USA
tsujimot@astro.psu.edu*

²*Department of Physics, Graduate School of Science, Kyoto University,
Kitashirakawa Oiwake-cho, Sakyo-ku, Kyoto, 606-8502*

³*Institute of Astronomy, University of Tokyo, 2-21-1 Osawa, Mitaka, Tokyo, 181-0015*

⁴*National Astronomical Observatory of Japan, 2-21-1 Osawa, Mitaka, Tokyo, 181-0015*

⁵*Department of Physics, Faculty of Science and Engineering, Chuo University,
1-13-27 Kasuga, Bunkyo-ku, Tokyo, 112-8551*

⁶*National Radio Astronomy Observatory, 1003 Lopezville Road, Socorro, NM 87801, USA*

(Received ; accepted)

Abstract

Using the Very Large Array (VLA) in the A-configuration, we have obtained a high-resolution 3.6 cm map of a hard X-ray source detected by the Chandra X-ray Observatory in a protostellar clump in Orion molecular cloud 3. Two radio continuum sources were detected in the vicinity of the X-ray source, both of which have NIR counterparts. We conclude that these VLA sources are free-free emission produced by shocks in protostellar jets from the NIR class I protostars. Using the centimeter data, we determined the power and orientation of the protostellar jets. The center position of the X-ray emission was found to be $\sim 1\text{--}2''$ offset from the exciting sources of the jets, and the displacement is in the direction of the jets and molecular outflows. We discuss the nature of the X-ray emission as the shock-excited plasma at the shock front where the jet propagates through interstellar medium at a speed of $\sim 1000\text{ km s}^{-1}$.

Key words: ISM: jets and outflows—radio continuum: ISM—X-rays: stars—stars: pre-main sequence

1. Introduction

Since the discovery of X-ray emission from star-forming regions (SFRs) using the Einstein Observatory in the 1980's (Feigelson, DeCampli 1981; Montmerle et al. 1983), low-mass young stellar objects (YSOs) have been known to be strong X-ray emitters. Subsequent X-ray observatories further revealed that almost all low-mass YSOs in the class I—III evolutionally stages emit X-rays and the emission originates from optically-thin thermal plasma with fast rises and slow decays in flux. These lead to the general consensus that X-rays from low-mass YSOs are attributable to high temperature ($T=10^6\text{--}10^7\text{ K}$) plasma maintained by occasional flares that are triggered by magnetic reconnections (see a review by Feigelson, Montmerle 1999).

Recent long-exposure observations by the Chandra X-ray Observatory are beginning to reveal new X-ray-emitting phenomena in SFRs with its unprecedented sensitivity and spatial resolution. These include the X-ray detection from a Herbig-Haro object (Pravdo et al. 2001) and the discovery of diffuse X-ray emission from high-mass SFRs (e.g., Townsley et al. 2003).

We conducted a $\sim 100\text{ ks}$ observation on Orion molec-

ular clouds 2 and 3 (OMC-2/3; $D=450\text{ pc}$) with the Advanced CCD Imaging Spectrometer (ACIS) onboard Chandra (Tsuboi et al. 2001; Tsujimoto et al. 2002a) in conjunction with deep near-infrared (NIR) follow-up imaging using the University of Hawaii 88 inch telescope (Tsujimoto et al. 2003). Among 385 X-ray detections, we found that $\sim 72\%$ sources have a NIR counterpart while the remaining sources have none. Based on the X-ray spectral and temporal properties as well as the spatial distribution and the K -band luminosity function of these sources, we concluded that most of the NIR-identified and NIR-unidentified X-ray sources are YSOs and background active galactic nuclei, respectively.

Among the NIR-unidentified X-ray sources, however, a few coincide spatially with the string of protostellar clumps in OMC-3 (MMS 1–10) seen in 1.3 mm continuum emission (Chini et al. 1997). The hard X-ray emission (source No. 8 in Tsuboi et al. 2001; we hereafter call this source TKH 8) detected at the protostellar clump MMS 2 is one of these peculiar X-ray sources. Its associations with the protostellar clump, with molecular outflows in CO, HCO⁺ (Aso et al. 2000; Williams et al. 2003), and shock-excited H₂ (Tsujimoto et al. 2002b) emission lines, and with protostellar jets in centimeter continuum (Reipurth et al. 1999), make this source unlikely to be a background

source. It is also unlikely that this X-ray emission is from the magnetic activity of a low-mass class I–III objects because the X-ray emission is centered at a position that is significantly ($\sim 1\text{--}2''$) offset from the closest NIR sources (IRS 3 and IRS 5; Tsujiimoto et al. 2002b). These results lead Tsuboi et al. (2001) and Tsujiimoto et al. (2002b) to speculate that this X-ray emission is from a hidden class 0 protostar, which is invisible by definition at NIR wavelengths (Barsony 1994).

We have carried out the highest-resolution centimeter imaging observation yet of TKH 8 using the Very Large Array (VLA) to investigate further the nature of this peculiar source. Given the fact that most protostars show free-free emission originating from protostellar jets (Rodríguez et al. 1995; André 1996), long-baseline interferometer imaging at centimeter wavelengths is the most accurate method of determining the position of jet-exciting sources, and the strength and orientation of the jet at its root. A D-configuration observation has already detected a 3.6 cm source at TKH 8 (Reipurth et al. 1999), although its coarse spatial resolution is insufficient to match the Chandra image. In this paper, we report the result of our A-configuration VLA observation of TKH 8, based on which we present another interpretation of the X-ray emission.

2. Observation & Result

We observed TKH 8 with the VLA of the National Radio Astronomy Observatory (NRAO) on February 11, 2002. We used the A-configuration to achieve sufficient spatial resolution to match that of the Chandra image. A 3.6 cm map was obtained with an integration time of ~ 3.5 hours and the phase center at R. A. = $05^{\text{h}}35^{\text{m}}18^{\text{s}}.3$, Decl. = $-05^{\circ}00'33''$ (J2000.0). The map is sensitive to structure smaller than $\sim 2''$ with an angular resolution of $\sim 0''.1$. This enables us to have a much finer view of the X-ray emission and its vicinity compared to the prior D-configuration observation, which had a resolution of $\sim 8''$ (Reipurth et al. 1999). 3C 48 (3.25 Jy) and 0541–056 (0.98 Jy) were used as the flux and phase calibrators, respectively.

Data reduction, calibration and analysis were performed using the Astronomical Image Processing System (AIPS). The naturally-weighted map is shown in figure 1. We detected two sources (VLA 1a and VLA 1b) above the 3σ level, for which we derived the position and the flux density (table 1). These two sources were not resolved in the prior D-configuration observation and were named altogether as VLA 1 (Reipurth et al. 1999). We detected $\sim 70\%$ of the total flux measured in the D configuration, indicating that we are missing some extended emission associated with VLA 1. VLA 1a is slightly extended, so we also determined the length of the major (minor) axis and position angle to be $0''.40$ ($0''.09$) and 32.2 degree, respectively. The direction of the elongation is shown with the arrow in figure 1.

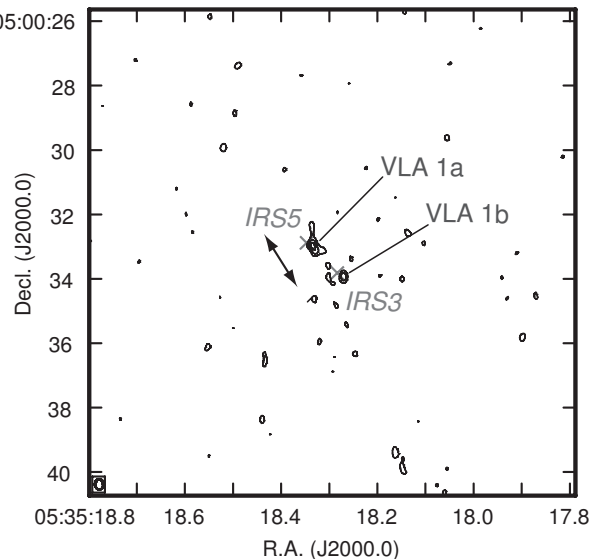


Fig. 1. The 3.6 cm intensity map (contours) with the position of the NIR sources (crosses). The position accuracy of the VLA sources are $\sim 0''.02$, while that of the NIR sources are $\sim 0''.1$. Contour levels are $3\text{--}9\sigma$ with a step of 3σ , where the background noise is $\sim 7.7 \mu\text{Jy beam}^{-1}$. The synthesized beam size is at the bottom left. The position angle of VLA 1a is shown with the arrow.

3. Discussion

3.1. The Origin of the Centimeter Emission

VLA 1a and VLA 1b are very close to the NIR sources IRS 5 and IRS 3, respectively (Tsujiimoto et al. 2002b). The apparent separation between IRS 5 and VLA 1a ($\sim 0''.1$) and between IRS 3 and VLA 1b ($\sim 0''.07$) are smaller than the NIR position uncertainty of $\sim 0''.1$. Thus, the NIR and radio sources are most likely coincident. Both IRS 3 and IRS 5 can be classified as class I protostars from their NIR excess and high extinction of $A_V > 50$ mag using the $(H-K)/(K-L')$ color-color diagram (figure 3b in Tsujiimoto et al. 2002b). The excess emission was also confirmed at the mid-infrared bands, securing the class I nature of these sources (Nielbock et al. 2003).

For the following four reasons, we conclude that both VLA 1a and VLA 1b are free-free emission from H_{II} regions ionized by the UV radiation from the shock front produced by a protostellar jet propagating through ambient matter (Curiel et al. 1987).

First, these centimeter sources are accompanied by class I protostars (IRS 3 and IRS 5). Embedded protostars are frequently associated with centimeter emission. Detailed studies indicate that most of these radio sources, if not all, are jet-induced free-free emission (Anglada 1996).

Second, IRS 3 and IRS 5 have the NIR magnitudes and colors of $J_0 > 11.3$ mag and $J-H > 1.6$ mag, and $J_0 > 11.3$ mag and $J-H > 3.8$ mag, respectively (Tsujiimoto et al. 2002b). This indicates that both sources have a mass less than $2 M_{\odot}$, which rules out the possibility that the centimeter emission is from H_{II} regions generated by

Table 1. Source list.

source ID	R.A. (J2000.0)	Decl. (J2000.0)	flux* (μJy)	NIR counterpart [†]
VLA 1a	05 ^h 35 ^m 18 ^s .335	-05°00'32".97	128±18	IRS 5
VLA 1b	05 ^h 35 ^m 18 ^s .271	-05°00'33".93	54±11	IRS 3

* The flux density is corrected for the primary beam response.

† The nomenclature follows Tsujimoto et al. (2002b).

stellar UV photons.

Third, the flux density multiplied by the square of the distance to the source from an observer ($S_\nu D^2$) and the momentum rate in the outflow (dP/dt) of VLA 1a and VLA 1b fit well with a known empirical relation (Anglada et al. 1992) and theoretical understanding (Curiel et al. 1987) of the jet-induced model. Figure 2 shows the relation between $S_\nu D^2$ and dP/dt for 16 embedded objects, where we added VLA 1a/b with $S_\nu D^2 = 0.182 \times 0.45^2 \text{ mJy kpc}^2$ (this work) and $dP/dt = 3 \times 10^{-5} M_\odot \text{ yr}^{-1} \text{ km s}^{-1}$ (Aso et al. 2000). Here, the limited spatial resolution of the HCO^+ and CO observations in Aso et al. (2000) did not resolve which of the three 1.3 mm clumps (MMS 2–MMS 4; Chini et al. 1997) is responsible for the molecular outflow. However, VLA 1a and VLA 1b in MMS 2 are the only 3.6 cm sources that are associated with MMS 2–MMS 4 (this work; Reipurth et al. 1999). We therefore safely assumed that the dP/dt value determined for this molecular outflow represents the sum of the momentum rate from VLA 1a and VLA 1b. Similarly, we summed the flux density of VLA 1a and VLA 1b for the S_ν value.

Fourth, in case of VLA 1a, the source is elongated (the arrow in figure 1) in the direction of the global outflow seen in the $\text{H}_2 v=1-0 \text{ S}(1)$ -band (Tsujimoto et al. 2002b; the main stream emanating from VLA 1a/1b in figure 3), which is characteristic of free-free centimeter emission induced by jets (Anglada 1996).

3.2. The Origin of the Hard X-ray Emission

The poor photon statistics of the hard X-ray source TKH 8 do not allow us to examine whether this is an extended source. However, with the assumption that it is a point-like source, the X-ray emission is significantly offset from the class I protostars (IRS 3 and IRS 5; Tsujimoto et al. 2002b). Our high-resolution radio map enables us to confirm that the displacement is in the direction of the jet and outflow. We discuss the origin of this X-ray emission together with the centimeter emission based on a jet-induced scenario.

Figure 4 shows a schematic view, where the hard X-rays are emitted from the post shock (PS) region, while the centimeter emission is from the recombination zone (RZ) behind the shock front. The RZ is maintained by the continuous ionization by UV photons from the PS region.

In PS, the temperature (T_{PS}) and the density (n_{PS}) are expressed as

$$T_{\text{PS}} = 1.5 \times 10^5 \left(\frac{v_s}{100 \text{ km s}^{-1}} \right)^2 \text{ [K]}, \quad (1)$$

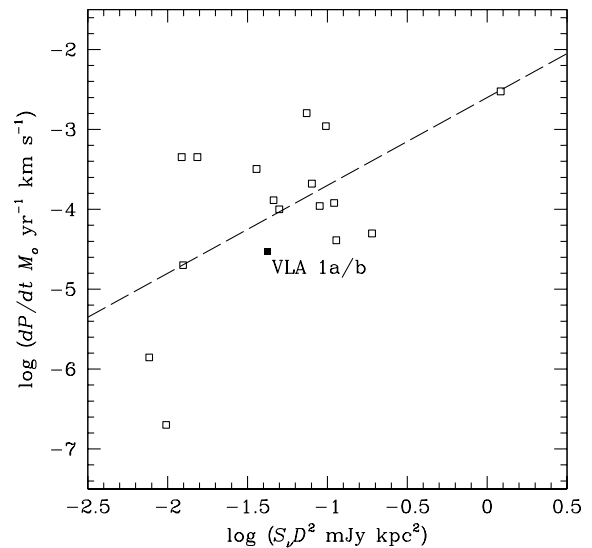


Fig. 2. Relation between $S_\nu D^2$ and dP/dt . Open squares are from Anglada et al. (1992), who derived an empirical relation for these sources (dashed line). VLA 1a/b (filled square) is consistent with this relation.

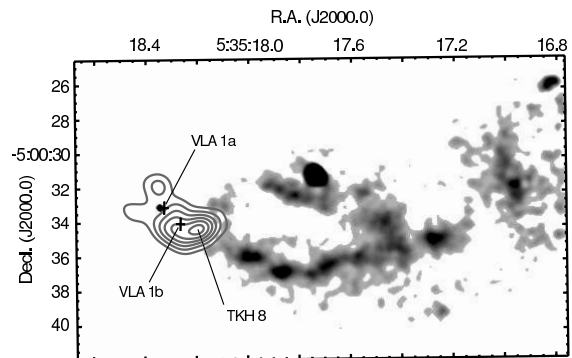


Fig. 3. The H_2 intensity map (gray scale) with the position of the 3.6 cm sources (pluses) and the hard X-ray intensity (contours).

$$n_{\text{PS}} = 4n_0 \text{ [cm}^{-3}\text{]}, \quad (2)$$

where v_s is the velocity of the shock produced by the collision of the jet into ambient matter with density n_0 (Raga et al. 2002). When v_s is large enough, we can expect to have X-ray emission from PS. Assuming that light elements are fully ionized in PS, the emission measure (EM) is given with the electron density (n_{PS}) and the volume (V_{PS}) of PS as

$$EM = n_{\text{PS}}^2 V_{\text{PS}} \text{ [cm}^{-3}\text{]}. \quad (3)$$

We fitted the X-ray spectrum of TKH 8 with an optically-thin thermal plasma model with the amount of interstellar absorption, plasma temperature, and emission measure as free parameters, obtaining an acceptable fit with $N_{\text{H}} = 12.7 \times 10^{22} \text{ cm}^{-2}$, $k_{\text{B}}T_{\text{PS}} = 3.05 \text{ keV}$, and $EM = 2.1 \times 10^{53} \text{ cm}^{-3}$. Readers should note, however, that these parameters are not well constrained due to the poor X-ray photon statistics of this source, which can bring a large uncertainty in the following calculations. Using the best-fit values, we derive $v_s = 1.5 \times 10^3 \text{ km s}^{-1}$ and $n_0 = 5.8 \times 10^2 \text{ cm}^{-3}$. Here, we assumed that PS is a cube at a distance of 450 pc with the length of $0.''5$ (= the pixel scale of ACIS).

The radio observations give us another constraint on the values of v_s and n_0 as shown below. In RZ, the centimeter intensity (S_ν) is given by

$$\left(\frac{S_\nu}{\text{mJy}}\right) = 1.42 \times 10^2 \left(\frac{\theta_a \theta_b}{\text{arcsec}^2}\right) \left(\frac{\nu}{5 \text{ GHz}}\right)^2 \times \left(\frac{T_{\text{RZ}}}{10^4 \text{ K}}\right) \{1 - \exp(-\tau_\nu)\}, \quad (4)$$

where θ_a and θ_b are the axis lengths of the extended centimeter source and T_{RZ} is the temperature in RZ (Curiel et al. 1993). The term $1 - \exp(-\tau_\nu)$ approaches τ_ν in the optically-thin limit, which is expressed in terms of the shock parameters (Curiel et al. 1989) as

$$\tau_\nu = 1.55 \times 10^{-7} \left(\frac{n_0}{1 \text{ cm}^{-3}}\right) \left(\frac{v_s}{100 \text{ km s}^{-1}}\right)^{1.68} \times \left(\frac{\nu}{5 \text{ GHz}}\right)^{-2.1} \left(\frac{T_{\text{RZ}}}{10^4 \text{ K}}\right)^{-0.55}. \quad (5)$$

By substituting the observed values for VLA 1a ($\nu = 8.3 \text{ GHz}$, $S_\nu = 0.128 \text{ mJy}$, $\theta_a = 0.''40$, and $\theta_b = 0.''09$) as typical values and assuming that $T_{\text{RZ}} = 10^4 \text{ K}$, we obtain

$$\left(\frac{n_0}{1 \text{ cm}^{-3}}\right) \left(\frac{v_s}{100 \text{ km s}^{-1}}\right)^{1.68} = 1.7 \times 10^5. \quad (6)$$

From the X-ray observations, we can independently derive that

$$\left(\frac{n_0}{1 \text{ cm}^{-3}}\right) \left(\frac{v_s}{100 \text{ km s}^{-1}}\right)^{1.68} = 5.7 \times 10^4. \quad (7)$$

These values are in a good agreement with each other within a factor of a few, supporting the protostellar jet scenario for the origin of the X-ray and centimeter emission.

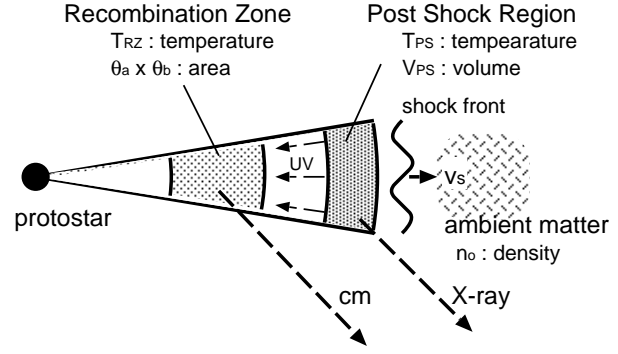


Fig. 4. Schematic view of the centimeter and X-ray emission at the shock front.

3.3. A Similar Example

Similar X-ray emission was recently reported by Bally et al. (2003) from L1551 IRS 5, in which an X-ray source detected by Chandra is located at the base of the protostellar jet. They argued three possibilities as the origin of the X-rays, including X-rays from fast shocks. Applying our scenario to this source using the X-ray observables given in Bally et al. (2003) and the centimeter observables in Cohen, Bieging, Schwartz (1982), we found that the discussion in Sect. 3.2 also holds for this source with $v_s \sim 500 \text{ km s}^{-1}$. This velocity is reinforced by Pyo et al. (2002), who present NIR echelle spectroscopy results on the $[\text{Fe II}]$ outflow from this source, and indicate the existence of a high velocity component reaching $400\text{--}500 \text{ km s}^{-1}$.

A recent series of works using $[\text{Fe II}]$ spectroscopy detected a highly-collimated high velocity component exceeding $\sim 200 \text{ km s}^{-1}$ in protostar outflows, including DG Tau ($250\text{--}300 \text{ km s}^{-1}$; Pyo et al. 2003) and HL Tau ($\sim 250 \text{ km s}^{-1}$; T-S. Pyo, private communication). In optical jet observations, FS Tau B was measured both in radial velocity and proper motion, giving a jet velocity of $\sim 400 \text{ km s}^{-1}$ (Eisloffel & Mundt 1998). Future X-ray observations of these systems with active jets are needed, to enrich the sample and examine the correlation between X-ray and centimeter observables, in order to test our idea.

3.4. Implications

Protostellar jets at a speed of $500\text{--}1000 \text{ km s}^{-1}$ may sound extreme. However, such a high velocity should not be surprising if we consider that even a Herbig-Haro object, which is far away from its powering source, is emitting X-rays induced by a $\sim 200 \text{ km s}^{-1}$ shock (Pravdo et al. 2001), and also that solar coronal mass ejections are frequently observed to be propagating at $\gtrsim 1000 \text{ km s}^{-1}$ (e.g., Gallagher et al. 2003). The lack of detection of $500\text{--}1000 \text{ km s}^{-1}$ jets so far does not prove their non-existence but simply means we have had no tools to measure them.

If this picture is established, we will obtain a strong method to derive the speed of highest velocity component of protostellar jets from X-ray imaging-spectroscopy using

equation (1), with no dependence on the inclination angle unlike proper motion or Doppler shift measurements. We consider more observations of similar sources will boost our understanding of this phenomenon, and eventually, of forming stars.

4. Summary

- We have made a high-resolution 3.6 cm imaging observation of a hard X-ray emission source (TKH 8) associated with a protostellar clump (MMS 2) in OMC-3 with the VLA. Two VLA sources were detected, both of which have the NIR counterparts.
- The centimeter emission is concluded to be free-free emission produced by a protostellar jet based on (1) the association with class I protostars, (2) the low-mass nature of these protostars, (3) the relation between the centimeter flux density and the momentum rate of the outflow, and (4) the elongated structure aligned with the global outflow.
- The hard X-ray source is located $\sim 1\text{--}2''$ offset in the direction of the protostellar jet and outflow from the NIR sources. The origin of the hard X-ray emission was discussed in the framework of jet-induced shocks. The X-ray and the centimeter observations give independent constraints on the shock parameters, which are found to be consistent with each other.

We would like to thank Tae-Soo Pyo for updated information on fast outflow observations. M. T. and N. K. express gratitude for the hospitality of NRAO staff in the Array Operation Center in Socorro, New Mexico, USA. The National Radio Astronomy Observatory is a facility of the National Science Foundation operated under cooperative agreement by Associated Universities, Inc. M. T. is financially supported by Japan Society for the Promotion of Science. K. K. is supported by a Grant-in-Aid for the 21st Century COE “Center for Diversity and Universality in Physics”.

References

André, P. 1996, in ASP Conf. Ser. 93, Radio Emission from the Stars and the Sun, ed. A. R. Taylor, & J. M. Paredes (San Francisco: ASP), 273

Anglada, G., Rodríguez, L. F., Cantó, J., Estalella, R., & Torrelles, J. M. 1992, *ApJ*, 395, 494

Anglada, G. 1996, in ASP Conf. Ser. 93, Radio Emission from the Stars and the Sun, ed. A. R. Taylor, & J. M. Paredes (San Francisco: ASP), 3

Aso, Y., Tatematsu, K., Sekimoto, Y., Nakano, T., Umemoto, T., Koyama, K., & Yamamoto, S. 2000, *ApJS*, 131, 465

Bally, J., Feigelson, E. D., & Reipurth, B. 2003, *ApJ*, 584, 843

Barsony, M. 1994, in ASP Conf. Ser. 65, Clouds, Cores, and Low Mass Stars, ed. D. P. Clemens and R. Barvainis (San Francisco: ASP), 197

Chini, R., Reipurth, B., Ward-Thompson, D., Bally, J., Nyman, L-Å, Sievers, A., & Billawala, Y. 1997, *ApJ*, 474, L135

Cohen, M., Bieging, J. H., & Schwartz, P. R. 1982, *ApJ*, 253, 707

Curiel, S., Cantó, J., & Rodríguez, L. F. 1987, *RMxAA*, 14, 595

Curiel, S., Rodríguez, L. F., Bohigas, J., Roth, M., & Cantó, J. 1989, *Ap. Lett. & Comm.*, 27, 299

Curiel, S., Rodríguez, L. F., Moran, J. M., & Canto, J. 1993, *ApJ*, 415, 191

Eisloffel, J. & Mundt, R. 1998, *AJ*, 115, 1554

Feigelson, E. D., & DeCampli, W. M. 1981, *ApJ*, 243, L89

Feigelson, E. D., & Montmerle, T. 1999, *ARA&A*, 37, 363

Gallagher, P. T., Lawrence, G. R., & Dennis, B. R. 2003, *ApJL*, 588, L53

Montmerle, T., Koch-Miramond, L., Falgarone, E., & Grindlay, J. E. 1983, *ApJ*, 269, 182

Nielböck, M., Chini, R., & Müller, S. A. H. 2003, *A&A*, in press

Pravdo, S. H., Feigelson, E. D., Garmire, G. P., Maeda, Y., Tsuboi, Y., & Bally, J. 2001, *Nature*, 413, 708

Pyo, T., Hayashi, M., Kobayashi, N., Terada, H., Goto, M., Yamashita, T., Tokunaga, A. T., & Itoh, Y. 2002, *ApJ*, 570, 724

Pyo, T. et al. 2003, *ApJ*, 590, 340

Raga, A. C., Noriega-Crespo, A., & Velázquez, P. F. 2002, *ApJ*, 576, L149

Reipurth, B., Rodríguez, L. F., & Chini, R. 1999, *AJ*, 118, 983

Rodríguez, L. F., Anglada, G., & Raga, A. 1995, *ApJ*, 454, L149

Townsley, L. K., Feigelson, E. D., Montmerle, T., Broos, P. S., Chu, Y., & Garmire, G. P. 2003, *ApJ*, 593, 874

Tsuboi, Y., Koyama, K., Hamaguchi, K., Tatematsu, K., Sekimoto, Y., Bally, J., & Reipurth, B. 2001, *ApJ*, 554, 734

Tsujimoto, M., Koyama, K., Tsuboi, Y., Goto, M., & Kobayashi, N. 2002a, *ApJ*, 566, 974

Tsujimoto, M., Koyama, K., Tsuboi, Y., Chartas, G., Goto, M., Terada, H., Kobayashi, N., & Tokunaga, A. T. 2002b, *ApJ*, 573, 270

Tsujimoto, M., Koyama, K., Kobayashi, N., Goto, M., Tsuboi, Y., & Tokunaga, A. T. 2003, *AJ*, 125, 1537

Williams, J. P., Plambeck, R. L., & Heyer, M. H. 2003, *ApJ*, 591, 1025